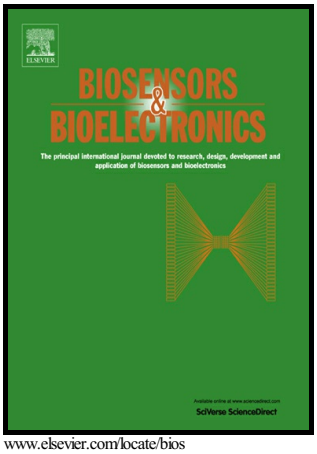

www.elsevier.com/locate/bios

Photoelectrochemical biosensor for HEN1 RNA methyltransferase detection using peroxidase mimics PtCu NFs and poly(U) polymerase-mediated RNA extension

Haiyan Wang, Libang Zhu, Junling Duan, Minghui Wang, Huanshun Yin, Po Wang, Shiyun Ai

PII: S0956-5663(17)30837-0
DOI: https://doi.org/10.1016/j.bios.2017.12.035
Reference: BIOS10180

To appear in: *Biosensors and Bioelectronic*

Received date: 8 October 2017
Revised date: 22 November 2017
Accepted date: 20 December 2017

Cite this article as: Haiyan Wang, Libang Zhu, Junling Duan, Minghui Wang, Huanshun Yin, Po Wang and Shiyun Ai, Photoelectrochemical biosensor for HEN1 RNA methyltransferase detection using peroxidase mimics PtCu NFs and poly(U) polymerase-mediated RNA extension, *Biosensors and Bioelectronic,* https://doi.org/10.1016/j.bios.2017.12.035

Photoelectrochemical biosensor for HEN1 RNA methyltransferase detection using peroxidase mimics PtCu NFs and poly(U) polymerase-mediated RNA extension

Haiyan Wang[†,a], Libang Zhu[†,a], Junling Duan [a], Minghui Wang [a], Huanshun Yin*[,a], Po Wang *[,b], Shiyun Ai

a College of Chemistry and Material Science, Shandong Agricultural University, Tai'an 271018, PR China

b School of Chemistry and Materials Science, Jiangsu Normal University, 221116, Xuzhou, Jiangsu, P.R. China

[†] These authors contributed equal to this work.

*Corresponding author.

E-mail: yinhs@sdau.edu.cn (Huanshun Yin), wangpo@jsnu.edu.cn (Po Wang).

Abstract: 2'-O-methyl group on the 3' terminal nucleotide in plant microRNAs, as one kind of RNA methylations, is caused by HEN1 RNA methyltransferase (HENMT1), which is thought to be crucial for ribosome biogenesis and function. Herein, a simple and label-free PEC biosensing method was proposed for assay of HENMT1 activity and inhibitor screening based on peroxidase mimic PtCu nanoframes (PtCu NFs) catalytic signal amplification. In this work, MoS_2@Graphene quantum dots/Phosphorus-doped rodlike carbon nitride (MoS_2@GQDs/P-RCN) heterojunction was used as photoactive materials. With the doping of GQDs and the formation of heterojunction, the photoactivity of MoS_2 is greatly improved. After the double-stranded RNA (dsRNA) with 2 nt 3' overhangs was treated with HENMT1 in the presence of *S*-adenosyl-*L*-methionine, the 3' terminal nucleotide of the unmethylated dsRNA could be extended under the catalysis of the poly(U) polymerase in the existence of UTP. Poly(A) nucleotide chain modified with carboxyl group was captured on the electrode surface through hybridization reaction and acted as a bridge for the immobilization of reticular DNA-functionalized PtCu NFs (PtCu@DNA). Under the catalysis effect of peroxidase mimics PtCu@DNA towards hydrogen peroxide, O^{2-} was *in situ* generated as electron donor and a strong photocurrent was obtained. The proposed PEC bioassay exhibited high selectivity and low detection limit of 3.36 ng/mL for HENMT1 activity assay. Furthermore, the inhibition research indicated that chlorpyrifos could inhibit the HENMT1 activity with the IC_{50} value of 48.32 nM.

Keywords: 2'-O-methyl group; HEN1 RNA methyltransferase; MoS_2@GQDs/P-RCN

heterojunction; Poly(U) polymerase; Peroxidase mimics PtCu nanoframes.

1. Introduction

HEN1 methyltransferase (HENMT1) catalyzes *S*-adenosyl-*L*-methionine (SAM)-dependent 2'-O-methylation at the 3'-termini of small double-stranded RNAs is a crucial factor in the biogenesis of plant small noncoding RNAs, such as microRNAs or siRNAs, which is first identified as a floral genes for the growing development of stamen and carpel identities (Chen et al. 2002). HENMT1 could recognize and methylate both miRNA/miRNA* and siRNA/siRNA* duplexes in vitro with a preference for 21-24 nt RNA duplexes with 2 nt 3' overhangs. HENMT1-mediated 2'-O-methylation has been demonstrated to be a key mechanism to protect plant microRNAs and small interfering RNAs as well as animal piwi-interacting RNAs from degradation and 3' terminal uridylation (Ren et al. 2012; Yu et al. 2005). Thus, it is reported that HENMT1 is closely associated with microRNA metabolism, and it is also been confirmed that microRNAs play fundamental roles in plant development (Park et al. 2002). Therefore, it is necessary to develop a method for HENMT1 detection. Up to now, most researches are focused on the action mechanism of HENMT1 and rarely explore its activity. Hence, it is meritorious for the assay of HENMT1 activity.

Photoelectrochemical (PEC) bioassays have attracted extensive attention in analytical community owing to its low background signal, excellent sensitivity,

portability (Cui et al. 2017; Dai et al. 2017a; Dai et al. 2016;). At present, due to the rapid development of nanoscience and nanotechnology, more attention has been concentrated on the design and applications of functional semiconductor species for innovative PEC biosensors (Li et al. 2017; Liu et al. 2017; Ong et al. 2017; Wang et al. 2017; Zhang et al. 2016; Zhou et al. 2017). MoS_2, a kind of 2D layered materials, is particularly attractive due to its narrow band gap (1.2-1.9 eV), the strong absorption in the visible light region, and large specific surface area (Wu et al. 2017). However, few studies on MoS_2-based PEC biosensing have been reported owing to the lack of surface functional groups and the limited photo response. Considering coupling quantum dots (QDs) with 2D layered materials to construct nanocomposite may provide a new kind of photoactive material with fast transfer and separation rate of photogenerated electron and hole. Graphene quantum dot (GQDs) with unique optical and electronic properties was doped with MoS_2 nanosheet for establishing a remarkable PEC biosensing platform with efficient separation of photogenerated electrons (e^-) and holes (h^+) pairs. Besides, fabrication of a heterostructure based on matchable energy levels has been demonstrated as an effective method for extending the absorbance to the visible region and enhance the separation process of photogenerated e^- and holes h^+ (Di et al. 2015; Li et al. 2015b). And various heterostructures has been applied onto PEC system, such as MoS_2/CdS (Lang et al. 2015; Zang et al. 2016), CQDs/TiO_2 (Tian et al. 2015), PbS QDs/NiO (Dai et al. 2017b), BiOBr/Ag_2S (Fan et al. 2017), Au/$BiVO_4$ (Shu et al. 2016) and so on. Phosphorus-doped rodlike carbon nitride (P-RCN), composing of only C, N, P and

some impurity H, exhibited excellent visible-light photoactivity, where P element doping narrows the band gap and prompt the charge separation (Guo et al. 2016). P-RCN possess large surface area-to-volume ratio, resulting the efficient electron transfer. P-RCN could be integrated by layer-by-layer assembly technique to construct the MoS_2-based heterostructures for improving the photoactive performance of MoS_2.

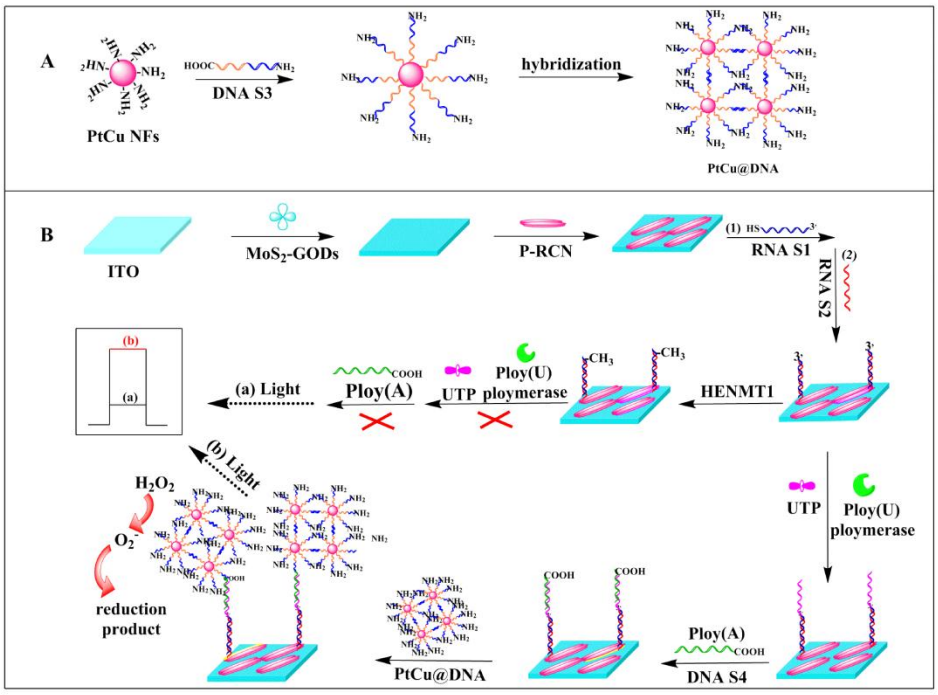

Scheme 1. Schematic representation of the preparation of PtCu@DNA (A) and the PEC biosensor construction process (B).

Pt-based alloys, used as peroxidase mimics, have emerged as highly stable and low-cost alternatives to natural enzymes. Importantly, five-fold-twinned PtCu nanoframes (NFs) have attracted increasing research interest due to its large surface area-to-volume ratio, 3D accessible surface and reduced consumption of noble metals. Inspiring by these investigations, we fabricated a novel PEC biosensor for assay of

HENMT1 activity based on MoS_2@GQDs/P-RCN heterojunction photoactive materials and PtCu NFs analogue enzyme. The fabricated process of the PEC biosensor was presented in Scheme 1. Carboxylated DNA S3 (at 5'-end) with a special sequences could be assembled on to the amino PtCu NFs surface, and then hybridization reaction was completed between these DNA S3 chains owing to the special sequences 5'-COOH-GAT AAG CAG CTG CTT ATC-NH_2-3', obtained reticular DNA-functionalized PtCu NFs and named (PtCu@DNA). The photoactive material of MoS_2 doped with GQDs (MoS_2@GQDs) was firstly coated on the bare ITO electrode surface through physical adsorption, and then P-RCN was further modified on it, forming heterostructures with MoS_2@GQDs, where P-RCN was not only as photoactivity substance to enhance the photoactivity of MoS_2@GQDs, but also as a bridge for probe RNA S1 immobilization. Based on the chemical reaction between thiol group of RNA S1 and amino group of P-RCN, probe RNA S1 was captured onto the modified ITO surface. When hybridization reaction was completed, RNA S2 was then adsorbed on the electrode surface, forming RNA duplexes with 2 nt 3' overhanging and away from the electrode surface. The formed dsRNA structure was suit for the latter poly(U) polymerase-mediated extension. Depending on the high exactitude of poly(U) polymerase, multiplex UTP was only incorporated into 3′ terminal RNA S1, obtaining the grown U-rich RNA. Then the completion of the hybridization reaction between A-rich DNA modified with carboxyl group and U-rich RNA leaded to the introduction of carboxyl group. Thereby, PtCu@DNA as the signal amplified unit was introduced onto ITO electrode surface through the reaction

between carboxyl group of DNA S4 and amino group of DNA S3. Due to the catalytic activity of PtCu NFs towards H_2O_2, O^{2-} was generated in situ and served as an electron donor in solution with the pH value of 7.4, resulting a strong photocurrent. Nevertheless, RNA duplexes with 2 nt 3' overhanging could also be specifically recognized by HENMT1 and methylated, and the methylated RNA could restrain the activity of poly(U) polymerase and protect the 3′ terminal RNA S1 from being extended. Thus, the followed processed could not be accomplished and the un-immobilization of the PtCu@DNA would lead to a weak PEC response. Therefore, the PEC signal was related to the methylation level and HENMT1 activity. In addition, this PEC biosensor was also applied to screen HENMT1 inhibitor.

2. Experimental

2.1 Materials and apparatus

Uridine-5'-triphosphate (UTP) was supplied by TriLink BioTechnologies, Inc. (San Diego, USA). Poly(U) Polymerase was obtained from New England BioLabs (USA). Disodium ethylenediaminetetraacetic acid (EDTA), tris (hydroxymethyl) aminomethane (Tris), sodium cholate (98%), DL-dithiothreitol (DTT), molybdenum (IV) sulfide (MoS_2 crystalline powder, <2 mm, 99%), melamine, copper (II) chloride dihydrate ($CuCl_2 \cdot 2H_2O$, 99%) and phosphorous acid were purchased from Aladdin Chemistry Co., Ltd. (Shanghai, China). Citric acid was acquired from Alfa Aesar (Lancashire, England). Chloroplatinic acid hexahydrate ($H_2PtCl_6 \cdot 6H_2O$, 99.5%), polyvinyl pyrrolidone (PVP, M_W = 40 000), sodium citrate, glycine (99%), sodium iodide (NaI, 99.5%), ethanolamine (99%), diethypyrocarbonate (DEPC),

ethanolamine were purchased from Sigma-Aldrich. Indium tin oxide (ITO) glass was obtained from Zhuhai Kaivo Electronic Components Co. Ltd., (China, ITO coating 180 ± 25 nm, sheet resistance <15 Ω/cm^2). HPLC-purified RNAs were obtained from Takara Biotechnology Co. Ltd. (Dalian, China). DNA probes were provided from by Sangon Biotech (Shanghai) Co., Ltd. The base sequences of the oligonucleotides were exhibited as follows: RNA S1, HS-5'-UGA AUG GAU GAU UCG GCA GCU GG-3', RNA S2, 5'- AGC UGC CGA AUC AUC CAU UCA-3', DNA S3, 5'-COOH- CTC CTC GTC GAA GAT AAG CAG CTG CTT ATC -3'-NH_2, DNA S4, COOH -5'- AAA AAA AAA AAA-3'. The transmission electron microscopy (TEM) images of the nanoparticles were acquired on a JEM-2010 transmission electron microscope (Japan). The UV-visible (UV-vis) absorption spectra were obtained on a UV-3600 UV-visible spectrophotometer (Shimadzu, Japan).

The buffers solution utilized in this work are as follows. TE buffer, 10 mM Tris–HCl, 1 mM EDTA, pH 8.0. RNA hybridization buffer, 1 × SSC (0.15 M sodium chloride and 15 mM sodium citrate). DNA immobilization buffer, 20 mM Tris–HCl, 2.0 mM EDTA, 2.0 M NaCl, and 2.0 mM TCEP, pH 7.0. DNA hybridization buffer, 10 mM Tris-HCl, 1.0 mM EDTA, and 1.0 M NaCl (pH 7.4). Washing buffer: 10 mM PBS (pH 7.4). 10 mM PBS was prepared by mixing the stock solution of 10 mM Na_2HPO_4 and 10 mM NaH_2PO_4. The pH was adjusted by 1 M HCl or 1 M NaOH. PEC determination buffer: 0.1 M PBS containing 400 nM H_2O_2. The redistilled deionized water used to prepare all solutions and was treated with DEPC.

2.2 Synthesis of MoS_2 nanosheets, GODs, P-RCN, PtCu NFs

MoS_2 nanosheets were synthesized according to previous report (Li et al. 2015a). In brief, 5 mg/mL MoS_2 powder and 1.5 mg/mL sodium cholate were mixed and sonicated at room temperature for 20 h, and then yellow-green dispersion was obtained. To remove bulk MoS_2, the resulting dispersion was centrifuged at 3000 rpm for 30 min. To isolate the prepared layer MoS_2, the yellow-green supernatant was centrifuged at 12,000 rpm for 30 min, the sediment was collected. In order to remove sodium cholate, MoS_2 nanosheets were dispersed in ultrapure water with the assistance of ultrasonication. Likewise, the resulting suspension was centrifuged at 12,000 rpm for 30 min, and this process was repeated for another two times to remove the sodium cholate completely. Finally, the prepared layer MoS_2 nanosheets were dispersed in redistilled deionized water.

The preparation of GQDs was completed according to previous paper (Dong et al. 2012). 2 g citric acid was put into a weighing bottle and heated to 200 °C in thermostatic drier oven. Approximately 5 min latter, citric acid was liquated, with the color of the liquid changing from colorless to pale yellow and then orange, resulting in the generation of GQDs.

For preparation of P-RCN (Guo et al. 2016), melamine (1 g) and phosphorous acid (1.2 g) were dissolved in 100 mL deionized water with magnetic stirring for 30 minutes, and the pH value of the mixture was 1.0. Afterwards, the mixture was transferred into a Teflon-lined autoclave which was maintained at 180 °C for 10 h. Then the mixture was collected by centrifugation, washed for three times with deionized water and dried at 60 °C. Ultimately, the products were heated to 500 °C for

4 hours using tube furnace under nitrogen atmosphere at a heating rate of 2.5 °C/min. The resulting material was designated as P-RCN.

In a typical procedure of PtCu NFs synthesis, 2 mmol glycine, 2 mmol NaI and 100 mg PVP were firstly dissolved into 3.65 mL of deionized water under strong stirring. Subsequently, 1 mL of 0.02 mM $H_2PtCl_6 \cdot 6H_2O$, 1 mL of 0.02 mM $CuCl_2 \cdot 2H_2O$ and 0.35 mL of ethanolamine were successively mixed with the above solution, with continuously stirring for 30 min at normal temperature. Afterwards, the homogeneous yellow-green solution was obtained, which was then transferred into a Teflon-lined autoclave and heated at 160 °C for 16 h. At last, the resulting suspension was centrifuged at 12,000 rpm for 10 min, and then the collected sediment was washed with deionized water and ethanol for three times, respectively. The obtained product was dispersed in ethanol. Then, −COOH of DNAS3 (2 μM, 20 μL) was activated by 20 μL of 0.1 M PBS (pH 7.4) containing EDC (0.5 mg/mL) and NHS (0.5 mg/mL) for 0.5 h, and then it was mixed with equal volume of PtCu NPs solution and kept for 2 h at 37 °C, the obtained product was named as PtCu@DNA.

2.3 Probe Immobilization and Hybridization

The ITO conductive glass substrates (5×1 cm^2) were thoroughly cleaned in an ethanol/NaOH mixed solution (v/v, 1:1) with sonication for 30 min, then acetone for 30 min and finally doubly distilled deionized water for 30 min and dried at room temperature. MoS_2@GQDs composites decorated ITO electrode (noted as MoS_2@GQDs/ITO) was fabricated primarily by dropping 40 μL of 1.5 mg/mL

MoS_2@GQDs onto the bare ITO slices and dried under an infrared lamp. Then, 40 μL of 1 mg/mL P-RCN dispersion was further dropped onto the MoS_2@GQDs/ITO electrode surface, dried under an infrared lamp irradiation and named as P-RCN/MoS_2@GQDs/ITO. Afterwards, thiol-capped probe RNA S1 (20 μL, 1.0 μM) was immobilized onto the P-RCN/MoS_2@GQDs/ITO electrode, allowing it to incubate at 37 °C for 2h, and then the modified electrode was washed by washing buffer for three times, and noted as ssRNA/P-RCN/MoS_2@GQDs/ITO. Subsequently, the hybridization reaction was completed by dropping 20 μL RNA hybridization buffer containing 1.0 μM complementary RNA S2 on the ssRNA/P-RCN/MoS_2@GQDs/ITO electrode surface and incubated for 2 h in a humid environment at 37 °C, obtaining dsRNA/P-RCN/MoS_2@GQDs/ITO electrode. After that, the modified electrode was rinsed three times with washing buffer to remove the un-hybridized complementary RNA from the electrode surface.

2.4 Poly(U) polymerase-mediated strand extension reaction and PtCu@DNA immobilization

Poly(U) polymerase-mediated strand extension reaction was carried out according to previous reports (Zhou et al. 2016). In a typical process, the obtained electrode was incubated with 20 μL poly(U) polymerase reaction buffer containing 30 U/mL poly(U) polymerase and 1 mM UTP at 37 °C for 75 min in a humid atmosphere, obtaining U-rich RNA/dsRNA/P-RCN/MoS_2@GQDs/ITO electrode. This process was followed by rinsing with washing buffer for three times. After that, 20 μL carboxyl-capped DNA S4 was further dropped onto the U-rich

RNA/dsRNA/P-RCN/MoS_2@GQDs/ITO electrode surface and hybridized with the ploy(U) strand of RNA, obtaining ds oligonucleotides/dsRNA/P-RCN/MoS_2@GQDs/ITO. Afterwards, 20 μL PtCu@DNA solution was dropped on the electrode surface and incubated for 30 min at 37 ^{o}C ambient temperature. After washing with washing buffer for three times, the fabricated electrode was noted as PtCu@DNA/ ds oligonucleotides/dsRNA/P-RCN/MoS_2@GQDs/ITO.

2.5 Methylation and Assay of HENMT1 Activity

The dsRNA/P-RCN/MoS_2@GQDs/ITO electrode was incubated with 20 μL HENMT1 reaction buffer with 160 μM SAM and various concentrations of HENMT1 at 37 °C for 2 h, followed by washing with washing buffer.

2.6 Inhibition of HENMT1 Activity

To investigate the inhibition effect of chlorpyrifos on the activity of HENMT1, methylation of dsRNA was performed in HENMT1 reaction buffer containing 160 μM SAM, 1 μg/mL HENMT1 and various concentrations of chlorpyrifos at 37 °C under a humid environment for 2 h. The inhibition percentage of chlorpyrifos was calculated with the equation of Inhibition (%) = $[(I_2-I_1)/(I_0-I_1)]\times100\%$, where I_0 was the photocurrent after the dsRNA treated with 0 μg/mL HENMT1, I_1 was the photocurrent of 1 μg/mL HENMT1 and I_2 was the inhibited photocurrent.

3. Results and discussion

3.1 Characterization of MoS_2 nanosheets, PtCu NFs, GODs and P-RCN

Fig. 1A shows a transmission electron microscope (TEM) image of the prepared

MoS_2, illustrating the nanosheet structure. The characterization of the as-prepared PtCu NFs is shown in Fig. 1B. As can been seen, the products are five-fold-twinned nanoframes with nanothorns protruding from the edges. The edge length and nanothorns length are about 60 nM and 10 nM, respectively, exhibiting the highly anisotropic feature. Although high quality TEM images of GQDs are difficult to be obtained due to the low electro contrast between the GQDs and the carbon coated TEM grids, some quantum dots of ~15 nm in size can still be observed (Fig. 1C). The ultraviolet-visible (UV-Vis) absorption spectra (Fig. 1D) of the GQDs shows a well-defined absorption band at 362 nm with a narrow full width at half maximum of 66 nm, which demonstrates that the sp^2 clusters contained in GQDs should be uniform in size. As illustrated in inset of Fig. 1D, a diluted aqueous GQD solution shows faint yellow color and gives blue light emission under the excitation by 365 nm UV light.

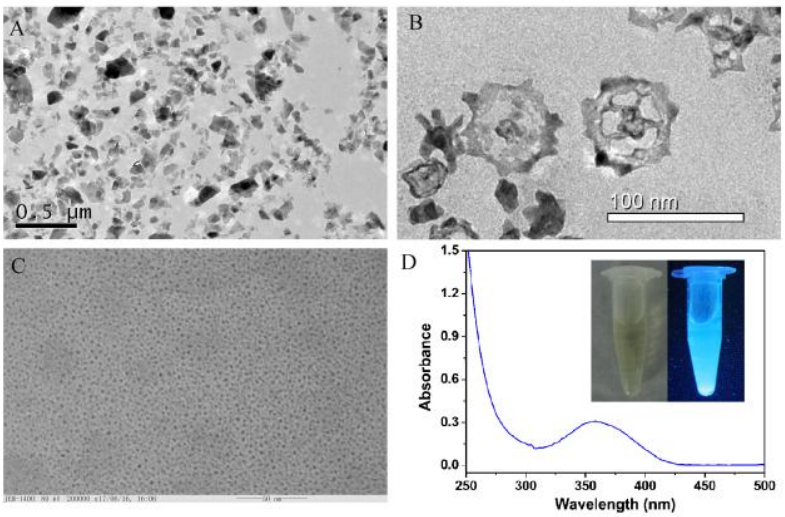

Fig. 1. TEM images of MoS_2 (A), PtCu NFs (B) and GQDs (C), (D) UV-Vis absorption of the GQDs, Inset: Photographs of the solution of GQDs taken under visible light (left) and 365 nm UV light (right).

3.2 EIS characterization

To monitor the fabrication process of the PEC immunosensor, the electrochemical impedance spectroscopy (EIS) was also performed at different modified electrodes in 5 mM $Fe(CN)_6^{3-/4-}$ solution. The EIS curves of the ITO at different modification steps were shown in Fig. 2. The EIS of the bare ITO revealed a relatively small semicircle domain (curve a). After coated with MoS_2@GQDs, the interfacial resistance significantly increased (curve b), confirming the successful immobilization of MoS_2@GQDs and it owns a high electronic conductivity. An increased R_{et} was observed when the surface was modified with P-RCN (curve c), suggesting the P-RCN was successfully immobilized onto the electrode surface and blocked the electron transfer. When the probe RNA S1 was captured on the modified ITO electrode, a remarkable increased R_{et} value was obtained (curve d), which could be explained that the electron transfer of the redox probe from solution to electrode was obstructed by the electrostatic repulsion between the negatively sugar-phosphoric acid backbone of RNA and redox probe. After the successive incubation of RNA S2 (curve e), Poly(U) ploymerase and UTP mixture (curve f), DNA S4 (curve g), the resistance was gradually increased, which was also attributed to the electrostatic repulsion between the negatively charged phosphate skeleton of nucleotides and $Fe(CN)_6^{3-/4-}$. Afterwards, the R_{et} value was further increased when the PtCu@DNA was assembled onto the electrode surface (curve h), which could be associated with the fact that the PtCu@DNA not only increased the steric hindrance, but also

suppressed the diffusion of the negatively charged of DNA S3 redox probe to the electrode surface. As a result, the PEC immunosensor has been fabricated successfully.

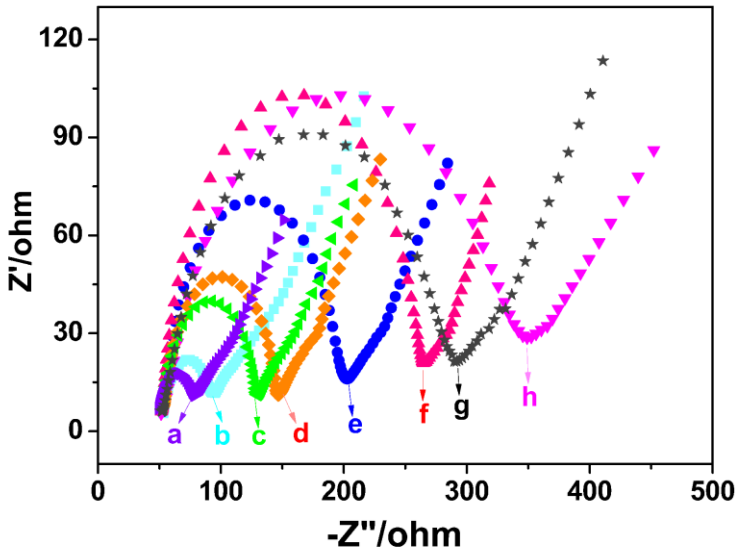

Fig. 2. EIS of the ITO under different condition in 5 mM $Fe(CN)_6^{3-/4-}$(1:1) solution containing 0.1 M KCl. (a) bare ITO, (b) MoS_2@GQDs/ITO, (c) P-RCN/MoS_2@GQDs/ITO, (d) ssRNA/P-RCN/MoS_2@GQDs/ITO, (e) dsRNA/P-RCN/MoS_2@GQDs/ITO, (f) U-rich RNA/P-RCN/MoS_2@GQDs/ITO, (g) ds oligonucleotides/dsRNA/P-RCN/MoS_2@GQDs/ITO, (h) PtCu@DNA/ds oligonucleotides/dsRNA/P-RCN/MoS_2@GQDs/ITO.

3.3 Detection feasibility assay

The feasibility assay of the experiment was completed by the comparing with the photocurrent of different biosensors. As illustrated in Fig. 3A, after deposition of MoS_2 (curve a) or GQDs (curve b) on the ITO slide, a PEC response was obtained,

which was lower than the photocurrent of MoS_2@GQDs/ITO. It could be explained that the doping of GQDs into MoS_2 could improve the photocurrent of pure MoS_2. As seen in Fig. 3B, when the ITO electrode was respectively modified with MoS_2@GQDs (curve a) and P-RCN (curve b), a weak photocurrent was observed. After the MG/ITO electrode coated with P-RCN, a relatively strong photocurrent was obtained (curve c), confirming that the MoS_2@GQDs and P-RCN heterojunction could enhance the photocurrent. However, the obtained photocurrent was still not enough strong due to the insufficient of the electron donor. Nevertheless, the PEC response decreased gradually when RNA S1 and complementary RNA S2 were successively assembled on the electrode surface (curve d), demonstrating that the transfer of the electron donor to the modified ITO surface for reacting with the photo-generated holes was hindered by those oligonucleotides. When the dsRNA/CN/MG/ITO electrode was successively incubated with the mixture of 30 U/mL poly(U) polymerase and 1 mM UTP, 1.0 μM DNA S4 and PtCu@DNA, the recorded photocurrent was significantly increased (curve e). It indicated that in the presence of PtCu NFs, H_2O_2 was hydrolyzed to produce the electron donor O^{2-}, which therefore caused in the observed increase of the photocurrent. In order to further verify that the methylation effect of HENMT1 could inhibit the poly(U) polymerase-mediated extension and lead to the decreased immobilization amounts of PtCu NFs, dsRNA/P-RCN/MoS_2@GQDs/ITO was successively incubated with 1 μg/mL HENMT1, 30 U/mL poly(U) polymerase and 1 mM UTP mixture, 1.0 μM DNA S4 and PtCu@DNA, the obtained photocurrent response (curve f) was close to

that of dsRNA/P-RCN/MoS_2@GQDs/ITO. On the basis of these results, one can conclude that this PEC biosensor could be used to analyze the HENMT1 activity.

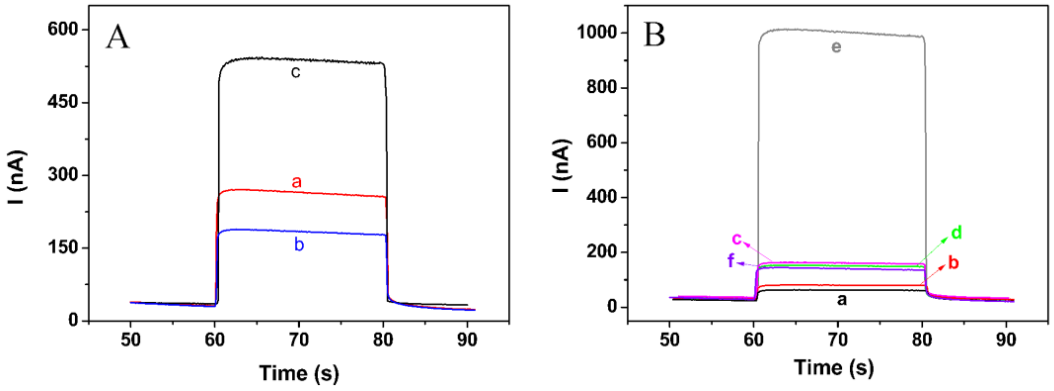

Fig. 3. (A) The photocurrent of (a) MoS_2/ITO, (b) GQDs/ITO and (c) MoS_2@GQDs/ITO in 0.1 M PBS (pH 7.4) containing 0.1 M AA. (B) The photocurrent of (a) MoS_2@GQDs/ITO, (b) P-RCN/ITO, (c) P-RCN/MoS_2@GQDs/ITO, (d) dsRNA/P-RCN/MoS_2@GQDs/ITO, (e) dsRNA/P-RCN/MoS_2@GQDs/ITO was incubated with 30 U/mL poly(U) polymerase and 1 mM UTP mixture, 1.0 μM DNA S4 and PtCu@DNA, successively. (f) dsRNA/P-RCN/MoS_2@GQDs/ITO was treated successively with 1 μg/mL HENMT1, 30 U/mL poly(U) polymerase and 1 mM UTP mixture, 1.0 μM DNA S4 and PtCu@DNA in 0.1 M PBS containing 400 nM H_2O_2.

3.4 Optimization of detection conditions

In order to improve detection efficiency, the effect of incubation time on the methylation level catalyzed by 1 μg/mL HENMT1 was explored. As exhibited in Fig. S2A (see Supplementary Materials), with extending the methylation time of HENMT1 from 10 to 60 min, the produced photocurrent decreased quickly, which

was accorded with the fact that more amount of dsRNA could be methylated by extending the methylation time of HENMT1. And then the photocurrent tended to level off at longer treatment time, implying that the methylation of dsRNA was nearly saturated. Thus, 60 min was used as the incubation time in this work. Besides, the concentration of MoS_2@GQDs and H_2O_2 were also investigated and were shown in supplementary material.

MoS_2@GQDs was acted as the photoactivity substrate, and its concentration was also expected to affect the detection sensitivity. As exhibited in Fig. S2B (see Supplementary Materials), the photocurrent increased with the MoS_2@GQDs concentrations increasing from 0.5 to 1.5 mg/mL and reached a maximum at 1.5 mg/mL. Thus, 1.5 mg/mL MoS_2@GQDs solution was selected as the optimal concentration.

H_2O_2-PtCu NFs system plays a crucial role in this PEC biosensing platform. Therefore, H_2O_2 concentration was a key parameter affecting the analytical performance with 1 μg/mL HENMT1. As can been seen from Fig. S2C (see Supplementary Materials), the photocurrent increased as H_2O_2 concentration increased from 50 to 400 nM, and reached a maximum at 400 nM. Therefore, 400 nM was selected as the optimum H_2O_2 concentration for this PEC detection. The P-RCN concentrations were also investigated. As displayed in Fig. S2D (see Supplementary Materials), 1.0 mg/mL was selected as the optimal condition.

3.5 Assay of HENMT1 Activity

The catalytic activity of HENMT1 was investigated by changing the HENMT1

concentration from 0.01 to 1 μg/mL. The assay process was carried out as described in section 2.4. As shown in Fig. 4A, the photocurrent gradually decreased with increasing HENMT1 concentration, which can be ascribed to the fact that the high concentration of HENMT1 could methylate more dsRNA to block the ploy(U) polymerase-mediated RNA extension reaction, which could decrease the capture amount of mimic enzyme PtCu@DNA. As presented in Fig. 4B, two regression equations of I = -1578.9473c + 884.211 (nA, μg/mL, R = 0.9865) and I = -562.5c + 712.5 (nA, μg/mL, R = 0.9786) were obtained with the concentration ranged from 0.01 to 0.2 μg/mL and from 0.2 to 1 μg/mL, respectively. The detection limit estimated from three times standard deviation of the blank measurements was to be 3.36 ng/mL.

The methylation selectivity was evaluated by testing M. SssI MTase, Dam MTsae. After complementary RNA S2 hybridized with RNA S1, the modified electrode was respectively incubated with 50 U/ml M. SssI MTase and 50 U/ml Dam MTase and maintained for 60 min. The PEC response was recorded and noted as I_1, and the change of the photocurrent ($\Delta I=I_0-I_1$) was compared, where I_0 represented the photocurrent of blank HENMT1. As illustrated in Fig. 4C, it was obvious that the ΔI the PEC response of M. SssI MTase and Dam MTase were similar and lower than that for 1 μg/mL HENMT1, which indicated that the photocurrent of interferents was closed to that of blank. It also suggested both M. SssI MTase and Dam MTase could not methylate the dsRNA and resulted in the success following modification processes. The result demonstrated that the biosensor had a satisfactory selectivity.

Fig. 4D displayed the reproducibility of the PEC biosensor. The reproducibility of the PEC biosensor was performed with the 1 μg/mL HENMT1 for seven detections based on freshly fabricated electrode. The RSD was 4.23%, implying an satisfactory detection reproducibility. The assay of stability was performed in Supplementary Materials.

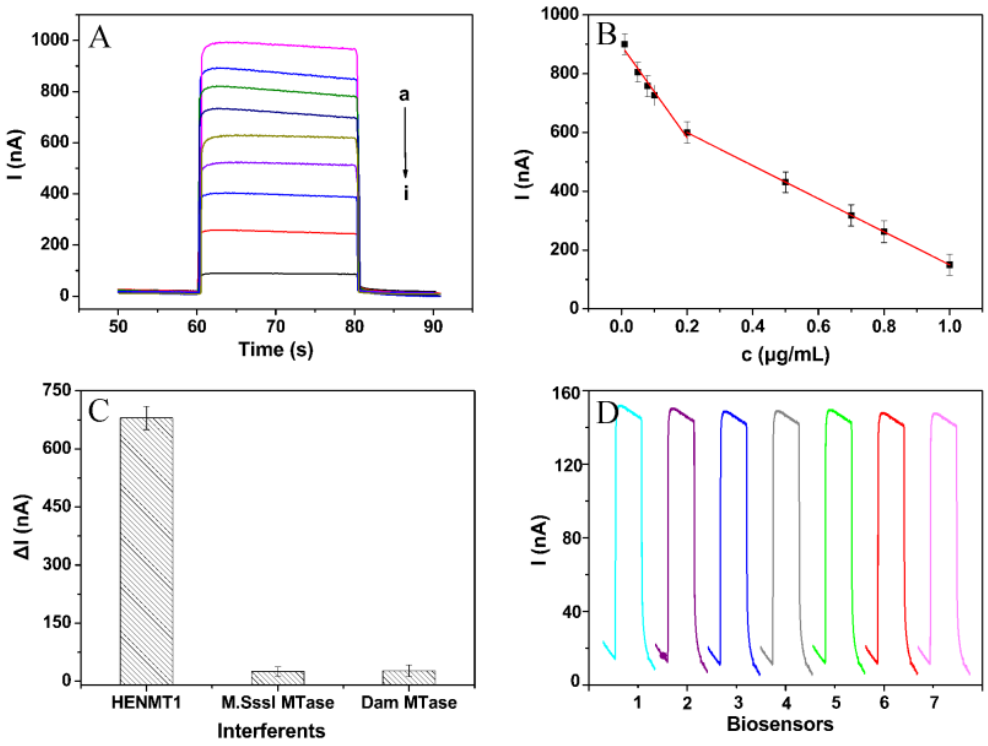

Fig. 4. (A) PEC response of the biosensor incubated with different concentration of HENMT1. a–i, 0.01, 0.05, 0.08, 0.1, 0.2, 0.5, 0.7, 0.8 and 1 μg/mL. (B) Calibration curve. The data was the average value of three detections. (C) The histogram for the photocurrent of the biosensors after incubated with different interferents. (D) PEC response of seven biosensors fabricated dependently.

3.6. The inhibition of chlorpyrifos on the HENMT1 activity

Many reports has demonstrated that the 2'-O-methylation could protect

microRNAs from degradation and 3'-end uridylation, which play crucial roles in gene regulations both in animals and plants (Huang et al. 2009; Saito et al. 2007). Therefore, it is important to discover the effect of pesticide on HENMT1 activity. Herein, in order to further confirm the application ability of the PEC strategy, the effect of chlorpyrifos (a kind of insecticide) on HENMT1 activity was investigated. As can been seen in Fig. 5, under the selected experimental conditions, the activity of HENMT1 was inhibited with increasing chlorpyrifos concentration, and the maximum inhibition efficiencies were 74.12% with the IC_{50} values of 48.32 nM. The result demonstrated that the PEC strategy was suitable to analyze the inhibition effects of pesticide on HENMT1 activity and screening HENMT1 inhibitors.

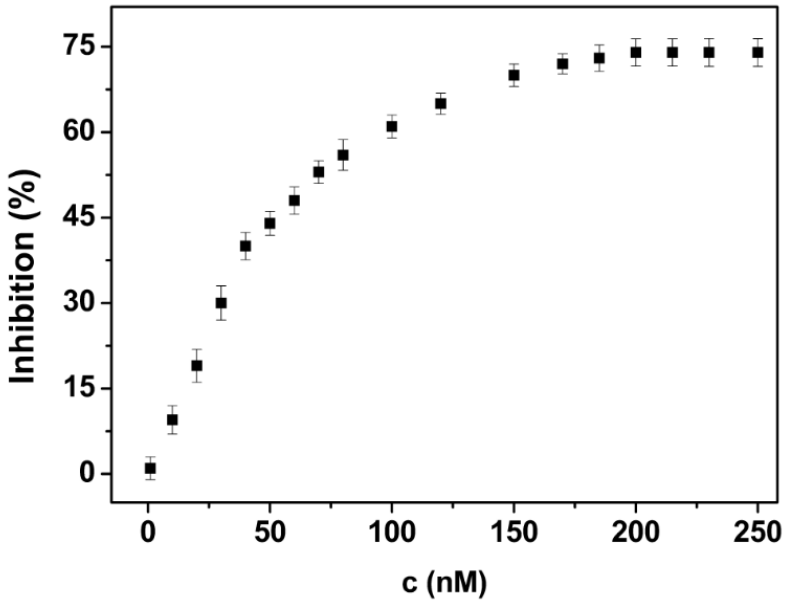

Fig. 5. The inhibition effect of chlorpyrifos on HENMT1 activity.

4. Conclusions

In summary, a simple and label-free PEC biosensing platform has been developed for HENMTI activity and inhibition assay based on MoS_2@GQDs/P-RCN

heterojunction photoactive materials, poly(U) polymerase mediated RNA extension reaction and peroxidase mimic PtCu@DNA catalytic signal amplification. With the assistance of signal amplifications, the proposed PEC biosensor presented an acceptable detection limit of 3.36 ng/mL. What is more, the PEC strategy was successfully applied for screening the HENMT1 inhibitor.

Acknowledgements

This work was supported by the Natural Science Foundation of Shandong province China (No. ZR2016BM10), the National Natural Science Foundation of China (Nos. 21775090, 21375079), Project of the Distinguished Young Scholar of Shandong Agricultural University, Founds of Shandong "Double Tops" Program (SYL2017XTTD15).

References

Chen, X., Liu, J., Cheng, Y., Jia, D., 2002. Development 129, 1085-1094.

Cui, L., Lu, M., Yang, X.-y., Tang, B., Zhang, C.-y., 2017. Analyst 142, 1562-1568.

Dai, H., Chen, S., Li, Y., Zeng, B., Zhang, S., Hong, Z., Lin, Y., 2017a. Biosens. Bioelectron. 92, 687-694.

Dai, H., Zhang, S., Hong, Z., Lin, Y., 2016. Anal. Chem. 88, 9532-9538.

Dai, W.-X., Zhang, L., Zhao, W.-W., Yu, X.-D., Xu, J.-J., Chen, H.-Y., 2017b. Anal. Chem. 89, 8070-8078.

Di, J., Xia, J., Ge, Y., Li, H., Ji, H., Xu, H., Zhang, Q., Li, H., Li, M., 2015. Appl. Catal. B-Environ. 168, 51-61.

Dong, Y., Shao, J., Chen, C., Li, H., Wang, R., Chi, Y., Lin, X., Chen, G., 2012.

Carbon 50, 4738-4743.

Fan, D., Wang, H., Khan, M.S., Bao, C., Wang, H., Wu, D., Wei, Q., Du, B., 2017. Biosens. Bioelectron. 97, 253-259.

Guo, S., Deng, Z., Li, M., Jiang, B., Tian, C., Pan, Q., Fu, H., 2016. Angew. Chem. Int. Edit. 55, 1830-1834.

Huang, Y., Ji, L., Huang, Q., Vassylyev, D.G., Chen, X., Ma, J.-B., 2009. Nature 461, 823.

Lang, D., Shen, T., Xiang, Q., 2015. ChemCatChem 7, 943-951.

Li, B.L., Zou, H.L., Lu, L., Yang, Y., Lei, J.L., Luo, H.Q., Li, N.B., 2015a. Adv. Funct. Mater. 25, 3541-3550.

Li, H., Yu, H., Quan, X., Chen, S., Zhao, H., 2015b. Adv. Funct. Mater. 25, 3074-3080.

Li, Y., Zhang, N., Zhao, W.-W., Jiang, D.-C., Xu, J.-J., Chen, H.-Y., 2017. Anal. Chem. 89, 4945-4950.

Liu, H., Weng, L., Yang, C., 2017. Microchim. Acta1-17.

Ong, W.-J., Putri, L.K., Tan, Y.-C., Tan, L.-L., Li, N., Ng, Y.H., Wen, X., Chai, S.-P., 2017. Nano Res. 10, 1673-1696.

Park, W., Li, J., Song, R., Messing, J., Chen, X., 2002. Curr. Biol. 12, 1484-1495.

Ren, G., Chen, X., Yu, B., 2012. Curr. Biol. 22, 695-700.

Saito, K., Sakaguchi, Y., Suzuki, T., Suzuki, T., Siomi, H., Siomi, M.C., 2007. Gene. Dev. 21, 1603-1608.

Shu, J., Qiu, Z., Lin, Z., Cai, G., Yang, H., Tang, D., 2016. Anal. Chem. 88,

12539-12546.

Tian, J., Leng, Y., Zhao, Z., Xia, Y., Sang, Y., Hao, P., Zhan, J., Li, M., Liu, H., 2015. Nano Energy 11, 419-427.

Wang, Y., Ge, S., Zhang, L., Yu, J., Yan, M., Huang, J., 2017. Biosens. Bioelectron. 89, 859-865.

Wu, S., Huang, H., Shang, M., Du, C., Wu, Y., Song, W., 2017. Biosens. Bioelectron. 92, 646-653.

Yu, B., Yang, Z., Li, J., Minakhina, S., Yang, M., Padgett, R.W., Steward, R., Chen, X., 2005. Science 307, 932-935.

Zang, Y., Lei, J., Hao, Q., Ju, H., 2016. Biosens. Bioelectron. 77, 557-564.

Zhang, N., Ruan, Y.-F., Ma, Z.-Y., Zhao, W.-W., Xu, J.-J., Chen, H.-Y., 2016. Biosens. Bioelectron. 85, 294-299.

Zhou, Q., Lin, Y., Shu, J., Zhang, K., Yu, Z., Tang, D., 2017. Biosens. Bioelectron. 98, 15-21.

Zhou, Y., Yin, H., Li, J., Li, B., Li, X., Ai, S., Zhang, X., 2016. Biosens. Bioelectron. 79, 79-85.

Graphic Abstract

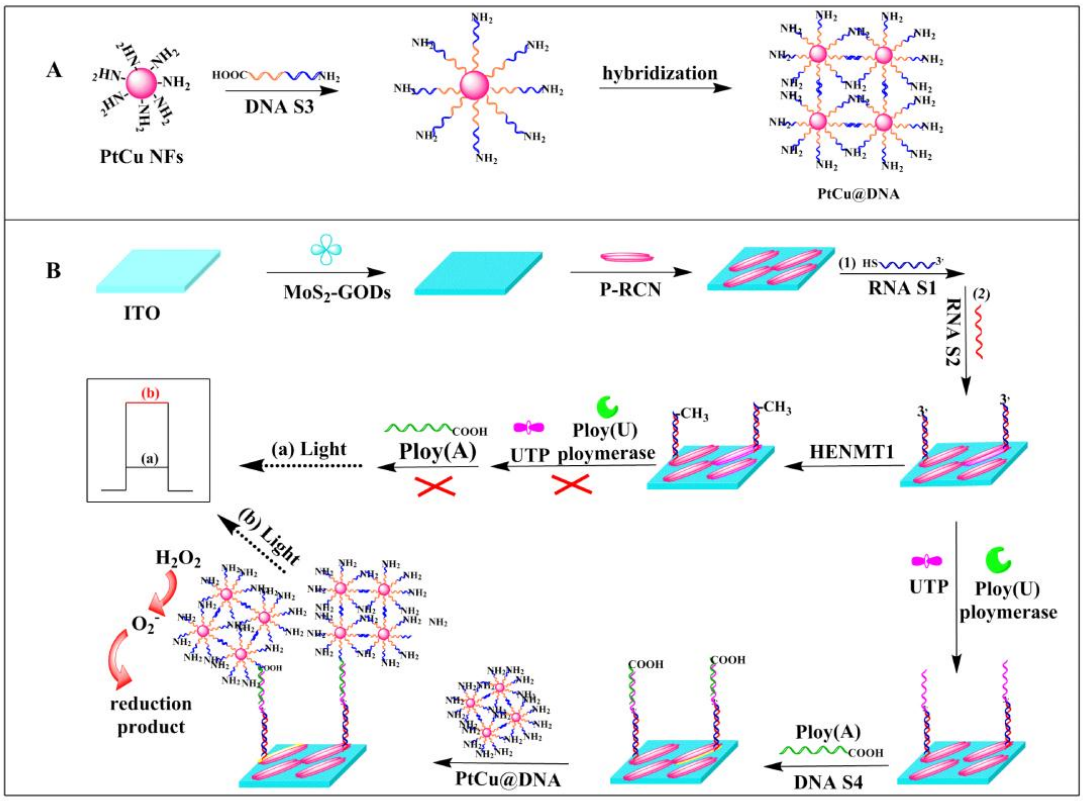

Highlights

- A simple and label-free photoelectrochemical strategy was developed for HEN1 RNA methyltransferase detection.
- MoS_2@Graphene quantum dots/Phosphorus-doped rodlike carbon nitride were used as photoactive materials.
- Five-fold-twinned PtCu nanoframes were used as peroxidase mimics and O^{2-} was *in situ* generated as electron donor.
- The photoelectrochemical biosensor was validated for detecting HENMT1 activity and screening HENMT1 inhibitor.